Backscattering-Based Measurement of Reactive Antenna Input Impedance

Backscattering-Based Measurement of Reactive Antenna Input Impedance

Pekka Pursula, Dan Sandström, and Kaarle Jaakkola

Abstract—A scattering technique for measuring reactive antenna input impedance is described. The antenna scattering is measured with three different loads: an open circuit, a conjugate match, and a reactive match. The load reactances tune the antenna into resonance at the measurement band. Theory and error considerations are presented, as well as measurement results of two ultra high frequency radio frequency identification antennas. The measurements were performed in a gigahertz transverse electromagnetic mode cell. The measured impedances are within about 10% of the simulated values for a dipole-like antenna. The results of a planar inverted-F antenna are somewhat more complex, but also supported by the presented simulations and the coaxial impedance measurement results.

Index Terms—Antenna impedance, backscattering, radio frequency identification (RFID), ultra high frequency (UHF).

I. INTRODUCTION

BACKSCATTERING-based antenna input impedance measurement techniques have been studied for decades [1], [2]. These techniques are not widely adopted, even though simple procedures with accurate results, like [3] and [4], have been reported. There are probably two reasons for this: 1) the scattering measurement in general requires sensitive instruments, and 2) in many cases, a feed-line connection to the antenna is needed to obtain results with sufficient accuracy. Recently, however, interest in backscattering measurements have increased, especially with radio frequency identification (RFID)-antennas, where the feed line connection to the antenna port is difficult to obtain. A backscattering-based radar cross-section measurement has been studied recently in [5], but the analysis was not developed far enough to extract the antenna input impedance from the backscattered signal.

In ultra high frequency RFID (UHF RFID), a capacitive integrated circuit (IC) is connected directly to an antenna. Optimizing the efficiency of the RF rectifier of the RFID chip has lead to highly reactive input impedances of the IC. Optimal operation of the transponder, or the tag, requires conjugate matching between the antenna and the IC, resulting in inductive antenna input impedances. The magnitude of reactance of the IC and the antenna can be even ten times higher than the resistance. Antennas like this cannot be simply connected to a 50 Ω feed line for input impedance measurement. A matching circuit could be used, but this does not remove the feed line, which affects the antenna behavior. In addition, the frequency behavior of the matching circuit differs from the behavior of the capacitive IC chip.

In the technique introduced in [3], the antenna scattering is measured with three resistive loads. The antenna input impedance is then calculated based on a linear three port model. The technique will be expanded for reactive load impedances, to measure the input impedance of an inductive antenna with a capacitive load. The technique perfectly fits to the measurement of UHF RFID antennas, because the capacitive loads are almost identical in frequency behavior to the load introduced by the RFID IC chip.

The advantage of proper loading cannot be overemphasized for two reasons: 1) since the antenna is tuned to resonance with the load, signal to noise ratio is optimized; and 2) the load of the antenna affects the antenna scattering in many unexpected ways, as will be seen later in this paper.

A scattering measurement is needed to measure the input impedance of a small reactive antenna; feed line measurements do not give accurate results, since the feed line couples strongly to the antenna and radiates as a part of the antenna. Especially this is a problem with small antennas, like RFID antennas, and with antennas whose feedpoint is not single-ended, e.g., planar inverted-F antennas (PIFAs) with small ground plane [6]. In the case of the technique to be introduced, no instrumentation other than a vector network analyzer is needed.

In the next section, the theory of the measurements is extended for reactive loads. After that, error analysis is presented. As an experimental verification, two reactive antennas are measured near 869 MHz in a gigahertz transverse electromagnetic mode (GTEM) cell. The measured antennas are specially designed RFID tag antennas for various applications. It is of great importance to be able to measure these antennas wirelessly in order to obtain information on their operation in different environments, and for a basis of their optimization. In Section V the measurement results are compared with simulations and coaxial feed line measurements.

II. THEORY

In this paper, we rely on the formulation developed by Harrington [2] and use the method described by Mayhan [3], with some exceptions. Harrington described the antenna under test (AUT), the receiving and transmitting antenna, as a linear three port network, which can be characterized with three impedance or admittance parameters. In this paper, the calculations are based on impedances, so these parameters are z_{rt}, z_{at} and Z_D. Subscript

r is for receiving and t for transmitting antenna respectively; z_{rt} describes coupling between receiving and transmitting antenna, and z_{at} coupling between transmitter and the AUT.

When the AUT is in the electric field of the transmitting antenna, it backscatters part of the incoming field. This scattered field is then received causing an excitation voltage at the receiving antenna. This relationship is, according to [2]

$$v_t \propto \left(z_{rt} - \frac{z_{at}^2}{Z_D + Z_L} \right) i_r \qquad (1)$$

where Z_D is the antenna input, or drive port, impedance of AUT and Z_L is the load impedance attached to the terminals of AUT.

To obtain Z_D from (1), which consists of three unknown parameters Z_D, z_{rt} and z_{at}, it is evident that three measurements with three different loads are needed. Mayhan [3] used a short circuit, an open circuit and a resistive load. Because of the reactive nature of RFID antennas, the short circuit was replaced with a capacitive load in order to achieve resonance at the desired frequency. For the same reason, the resistive load was replaced with a capacitor and resistor connected in series. These three different load are denoted by Z_c, Z_o and Z_m. Subscript c is for capacitive load, o for open circuit and m for matched load. The same subscripts are used for the measured scattered fields, denoted by V_c, V_o and V_m. They can be solved by substituting different load impedances into (1), resulting in

$$KV_o = z_{rt} \qquad (2)$$

$$KV_c = z_{rt} - \frac{z_{at}^2}{Z_D + Zc} \qquad (3)$$

$$KV_m = z_{rt} - \frac{z_{at}^2}{Z_D + Zm} \qquad (4)$$

where K is a dimensional constant. Substituting (2) into (3) and (4), results in a new set of equations

$$K(V_c - V_o) = \frac{-z_{at}^2}{Z_D + Z_c} \qquad (5)$$

$$K(V_m - V_o) = \frac{-z_{at}^2}{Z_D + Z_m}. \qquad (6)$$

Dividing (5) with (6) and solving for Z_D gives

$$Z_D = \frac{Z_m - AZ_c}{A - 1} \qquad (7)$$

where A contains the measured scattered fields, which can be associated with a relevant scattering parameter; in this paper a monostatic case is considered and thus S_{11} is used. Now A can be expressed as

$$A = \frac{S_c - S_o}{S_m - S_o}. \qquad (8)$$

III. ERROR ANALYSIS

The technique gives accurate results when the antenna mode scattering dominates over the structural mode scattering, which

holds for the rod antennas measured in [3] for a very wide band. In (1), the first term describes the structural mode scattering and the second term the antenna mode scattering [7]. The structural mode scattering neither depends on the load of the antenna nor the antenna input impedance, but the antenna structure, e.g., metal plates in PIFAs, scatter nevertheless. The other term describes antenna mode scattering, that depends on the antenna input impedance and load. The antenna mode scattering arises, because the structure works as an antenna, feeding power to the load. Hence, it is natural that the signal to noise ratio of the antenna input impedance measurement is at its maximum when the antenna mode dominates the scattering.

In Section II, the three different loads were chosen to be an open circuit, a capacitive load and a matched load. The value of the capacitor is based on the simulated antenna input impedance and is determined in Section V. The resistor value should be chosen so that it contributes to the total error as little as possible. Mayhan [3] listed various error sources in his article, but our interest is to find the optimal value for the resistor. When attaching different loads to the AUT, physical displacement errors occur. This error type is dominating in higher frequencies. The error is calculated using partial differentiation. Taking into account the phase shift when the AUT is removed for load attachments, we get

$$\Delta Z_D = \sum_i \left| \frac{\partial Z_D}{\partial S_i} \right| \Delta_i$$
$$= \sum_i \left| \frac{\partial Z_D}{\partial S_i} \right| \left(\frac{\partial S_i}{\partial |S_i|} \Delta_{|S_i|} + \frac{\partial S_i}{\partial \phi_i} \Delta_{\varphi_i} \right) \qquad (9)$$

where i refers to c, m and o. $\Delta_{|S_i|}$ stands for the residual background level after background cancellation methods have been used and Δ_{φ_i} is the phase shift caused by displacement. The background level can be estimated from the undulation of the S-parameter magnitude curves.

By denoting the displacement error as Δ_L, (9) takes the following form:

$$\Delta Z_D = \sum_i \left| \frac{\partial Z_D}{\partial S_i} \right| \left(\Delta_{|S_i|} + j4\pi \frac{\Delta_L}{\lambda} |S_i| \right) e^{j\varphi}. \qquad (10)$$

After some manipulation, an expression for the error as a function of measured scattering parameters is obtained

$$\Delta Z_D = \frac{(S_o - S_m)(Z_m - Z_c)}{(S_m - S_c)^2} \Delta_c + \frac{(S_o - S_c)(Z_m - Z_c)}{(S_m - S_c)^2} \Delta_m + \frac{(S_m - S_c)(Z_m - Z_c)}{(S_m - S_c)^2} \Delta_o. \qquad (11)$$

Assuming that the Δ-variables are uncorrelated, summation in (11) can be done quadratically. It is also assumed that the Δ-variables are equal and denote them as σ_B. The final form of the error estimate, denoted by σ_D^2, is thus

$$\sigma_D^2 = \sigma_B^2 |Z_m - Z_c|^2 \cdot \frac{|S_o - S_m|^2 + |S_o - S_c|^2 + |S_m - S_c|^2}{|S_m - S_c|^4}. \qquad (12)$$

In (12), σ_B^2 stands for the residual background level [see (9)]. The equation consists of differences between two S_{11}-parame-
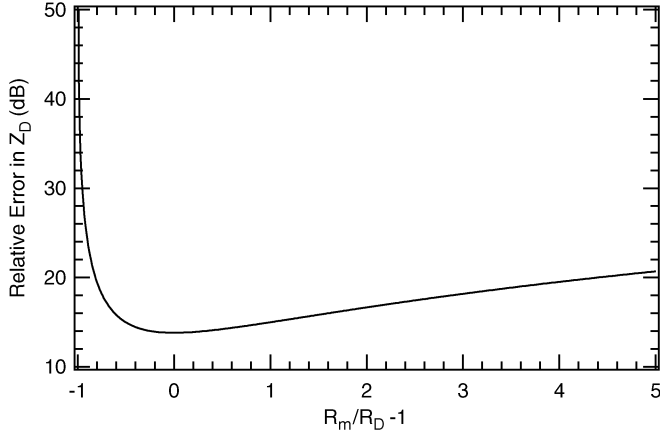
Fig. 1. Relative error in Z_D as a function of the load resistance R_m. Reactive matching is assumed perfect, and resistances $R_c = 0$ and $R_o = \infty$.
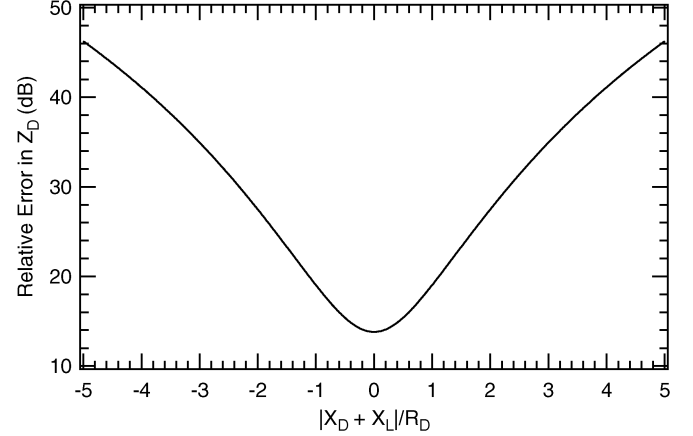

Fig. 2. Relative error in Z_D as a function of the reactive mismatch $|X_D + X_L|$, where load reactances $X_c = X_m = X_L$. Resistances $R_c = 0$, $R_m = R_D$ and $R_o = \infty$.

ters. Using (2)–(4), an expression can be derived for σ_D^2, that includes the different load impedances Z_c and Z_m

$$\sigma_D^2 = \frac{K^2 \sigma_B^2 R_D^4}{|z_{at}^2|^2} \left[\frac{|Z_D + Z_m|^2 |Z_D + Z_c|^2}{R_D^4} \right.$$
$$\left. \cdot \frac{|Z_D + Z_c|^2 + |Z_D + Z_m|^2 + |Z_m - Z_c|^2}{|Z_m - Z_c|^2} \right]. \quad (13)$$

The input resistance R_D has been introduced into the equation to make the bracketed term that describes the error as a function of the impedances unitless.

In order to determine the optimum choice for the load resistor in Z_m, the bracketed part of (13) was calculated at the resonant frequency by substituting different resistor values to the load Z_m. For simplicity, the reactive match is assumed to be perfect. The result is in Fig. 1. The smallest contribution to total error is achieved when the resistor value is chosen to be the same as the antenna input resistance.

The same kind of calculation can be made for reactive mismatch of Z_m and Z_c with respect to Z_D. Denoting the reactive part of Z_D as X_D and X_L as the reactive part of Z_i, $i = c, m$, we can use (13) and vary X_L. The result is in Fig. 2, from which we can see that the error related to reactive mismatch is at its minimum when the reactive part of Z_m and Z_c equals the reactive part of Z_D.

The error grows with increasing reactive and resistive mismatch. The loads can only be fully matched to the antenna at one frequency point. Hence, the error grows when leaving the antenna center frequency.

IV. ANTENNAS UNDER TEST

The transponder antenna is the most critical part of the system in many applications of passive UHF RFID. This is mostly because the performance of the antenna, realized as the maximum reading distance of the tag, tends to be affected by the mounting platform as well as the whole near environment of the tag. The two antennas measured, shown in Fig. 3, represent two types of UHF RFID tags.

The Palomar antenna [11] is a single-layer structure especially designed to be compact in size and to provide an almost
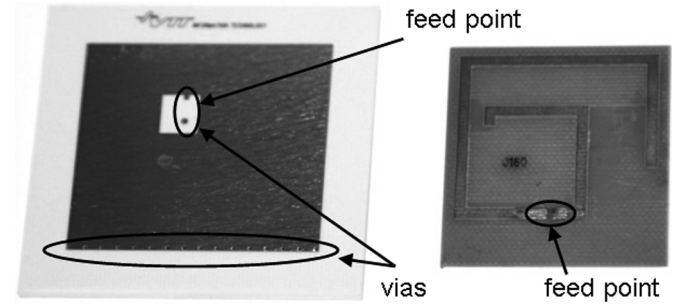

Fig. 3. The measured antennas: on the left the PIFA and on the right the Palomar antenna.

isotropic radiation pattern. This is due to its operation both as an electric and a magnetic dipole. The prototype measured has been fabricated by cut milling on a single-layer FR4 board. Because the antenna is a single-layer structure, it can also be manufactured inexpensively as a label using the most common technology of today's tag manufacturing.

The PIFA antenna [12] has been designed to be mounted on any surface, especially on metal that is practically impossible for direct mounting of a dipole-based label antenna. This antenna prototype has been realized using printed circuit board technology on a two-metal-layer panel of low-loss microwave material (RO4003). The size of the antenna is $60 * 60 * 3 \text{ mm}^3$. The short-circuiting contact between the layers of the antenna, which is required for the PIFA structure, has been implemented by a set of vias at one edge of the antenna patch. There is also a via connection at the feed point of the antenna. This type of tag antenna is more expensive to produce than the more common labels. Such antennas are typically used for recyclable tags in harsh environments, e.g., pallets and containers.

In the case of the Palomar antenna and similar structures, the measurement method concerned is of special importance. Because of its omnidirectional radiation pattern, the operation of the antenna is easily disturbed by any cable connected to it; thus the impedance reading would be inaccurate in such measurement. Theoretically, a PIFA-type antenna radiates in half-space and its feed impedance can be measured using a coaxial cable
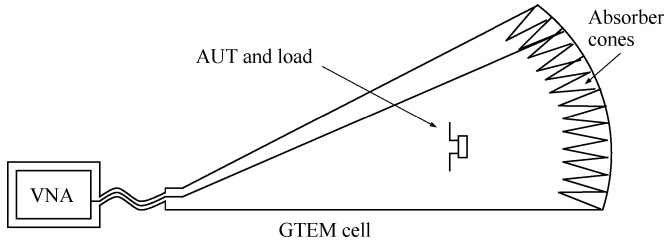
Fig. 4. Measurement setup. The scattering parameter S_{11} is measured with the vector network analyzer (VNA).

Fig. 5. Measured scattering parameters S_{11} of the Palomar antenna with different loads.

and tapped feed through the ground plane of the antenna. This has been done to the PIFA concerned for comparison, and the results are examined in the next section. Practical PIFA antennas have non-infinite ground plane, especially RFID tag antennas that have to be compact in size. Therefore, the coaxial cable feed does disturb the antenna.

V. MEASUREMENT RESULTS

To verify the theoretical results, the two antennas introduced in the previous section were measured with the technique. Both are designed for direct matching to a UHF RFID IC chip. The designed input impedance of the antennas is $(10 + j160)\ \Omega$ at 869 MHz. The inductive input impedance is matched by a capacitive load of 1 pF, i.e., a reactance of $-183\ \Omega$ at 869 MHz. A resistive load of 15 Ω for R_m was chosen because the relative error quickly rises, if $R_m < R_D$.

The measurements were carried out in a GTEM cell, described in [8]. GTEM cells have been used to measure radiation patterns [9] and gain of small antennas [10]. The GTEM cell is a waveguide, in which a plane wave propagates with TEM-mode. Thus the wave propagating in the cell is similar to a wave in free space. However, mismatch in wave and characteristic impedances has to be considered if absolute values of the scattered signals need to be determined, i.e., when measuring the antenna gain [10]. But, in our case, the input impedance of the antenna is calculated from relative scattered signals. In other words, the coupling constant K in (2)–(4) is not needed in (7) to calculate the input impedance.

The schematic of the measurement setup is presented in Fig. 4. The antenna under test (AUT) was positioned in the GTEM cell and the scattering parameter S_{11} measured with the vector network analyzer (VNA), which was connected to the feed point of the GTEM cell. The measurement was repeated with the three different loads connected to the AUT. The S_{11} of the empty GTEM cell was also measured; this was not needed to calculate the input impedance Z_D of the antenna, but only to present the change in S_{11} due to the different loads with the background subtracted.

Fig. 5 presents the measured magnitudes of the scattering parameter S_{11} of the Palomar antenna with four different loads. The load $Z_L = \infty$ describes the antenna structural mode. The capacitive and matching loads give rise to antenna mode, which dominates the structural mode in the application band.

An interesting phenomenon is observed with the capacitive load: if no series resistance is present, the antenna center frequency is shifted to higher frequencies and, more important, the
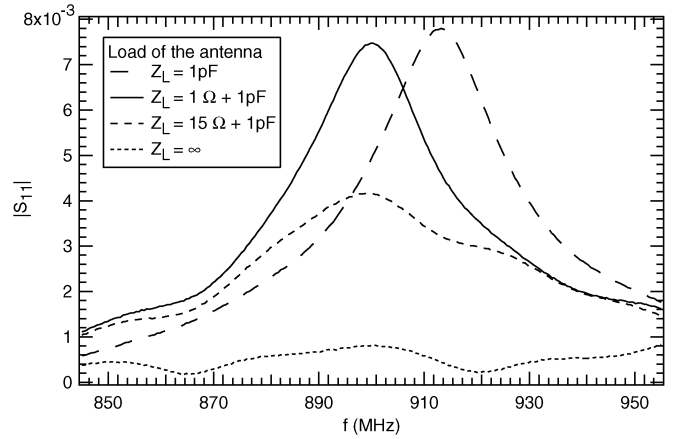
S_{11} of the capacitive load and the matching load cross. This leads to evident error in the input impedances, for Z_D diverges, when S_c equals S_m as seen from the (7).

The reason for this behavior was beyond the resources of the study but was probably due to the series inductance of the chip resistor. An empirical solution for the problem was found: By adding a small series resistance to the capacitive load, the center frequency remained at the center frequency of the matched load. Hence, loads $Z_o = \infty$, $Z_m = 15\ \Omega + 1\,\mathrm{pF}$ and $Z_c = 1\ \Omega + 1\,\mathrm{pF}$ were used.

Figs. 6 and 7, present the results of the Palomar antenna input impedance, as well as simulations with the HFSS software. In the case of the reactance, the opposite reactance of 1 pF at the center frequency of the scattering peaks in Fig. 5 is presented as this should be the antenna reactance at the frequency.

The error is smallest in the middle of the scattering peak, where the measured scattering parameters differ the most, as seen from (9). The error sources of the measurement setup were estimated as follows: The error in scattering parameter magnitude, or $\Delta_{|S_i|}$, was approximated as the ripple in the measured curves in Fig. 5. The repositioning error was approximated as 1 mm. In this case, the effect of the repositioning error was over an order of magnitude higher than the effect of the residual background. The resulting errors are presented in Figs. 6 and 7 as the gray area surrounding the measured value. As expected, the error grows as the difference between matched and shorted scattering parameters in Fig. 5 diminishes. Very accurate results are acquired at the resonance peak frequency.

The PIFA antenna was also measured with four loads, as seen in Fig. 8. In the open-circuited case the antenna self-resonance is seen at 910 MHz. Also here the resonance peak shift to higher frequencies with zero load resistance, and a series resistance of 1 Ω was added to the load Z_c. The resonance seems to have slightly different characteristics here than in the case of the Palomar antenna: the antenna mode scattering seems to add to the structural mode in anti-phase at frequencies below the resonance peak, resulting in scattering parameter amplitudes below the structural mode.

Figs. 9 and 10, present the results of the PIFA antenna input impedance, as well as simulations and a reference measurement:
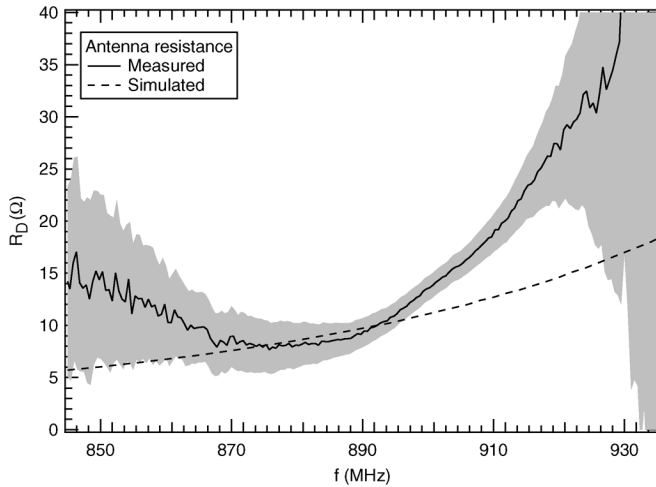
Fig. 6. Measured and simulated input resistances of the Palomar antenna. The gray area represents the error in the measured value.
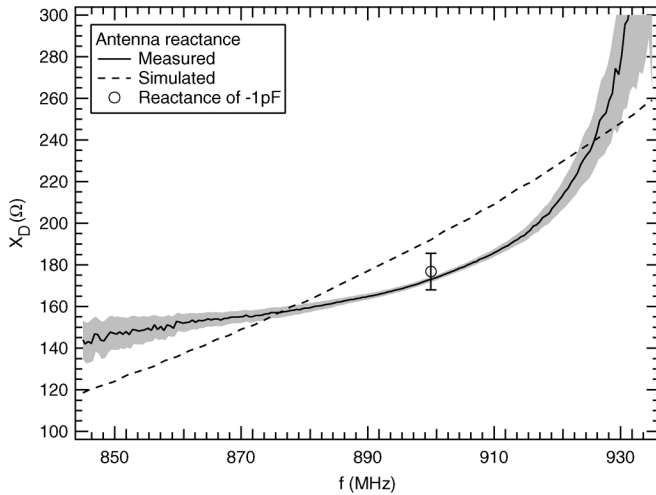

Fig. 9. Measured and simulated input resistances of the PIFA antenna. The gray area represents the error in the measured value.

Fig. 7. Measured and simulated input reactances of the Palomar antenna. The gray area represents the error in the measured value.
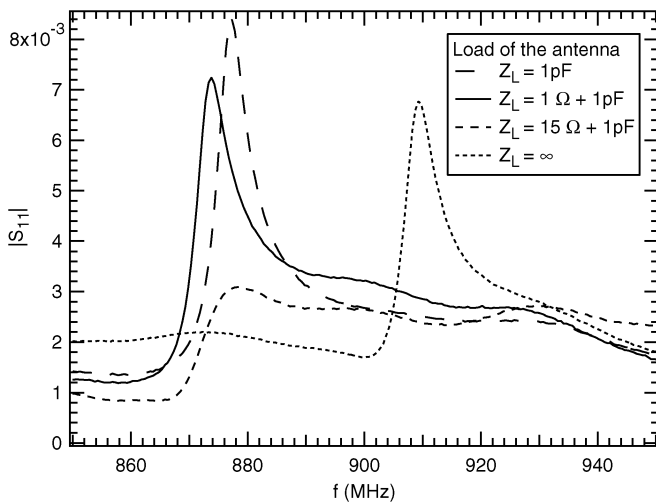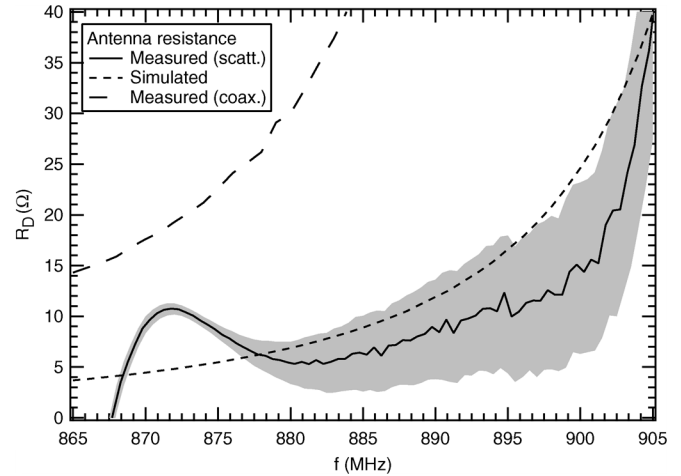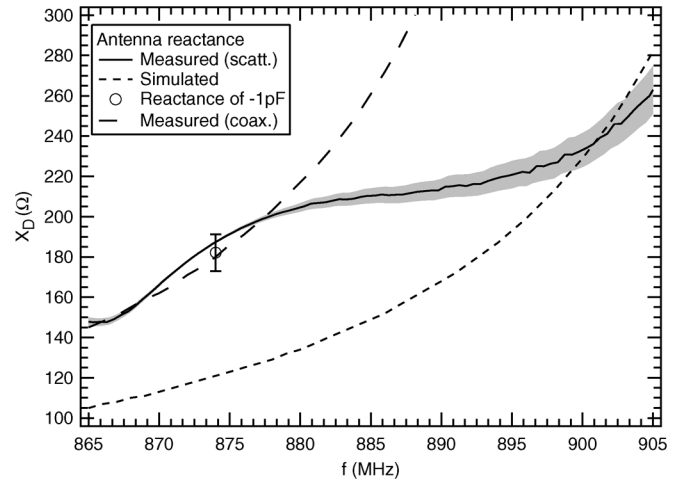

Fig. 10. Measured and simulated input reactances of the PIFA antenna. The gray area represents the error in the measured value.

Fig. 8. Measured scattering parameters S_{11} of the PIFA antenna with different loads.

A coaxial feed line was attached to the antenna feed point and the scattering parameter S_{11} measured with a VNA. The opposite reactance of 1 pF at the center frequency of the scattering peaks in Fig. 8 is also presented.

Immediately it is seen that the measurement result of the antenna resistance cannot be right at low frequencies, where negative values are obtained. This happens as shorted and matched scattering parameters sink below the structural mode scattering. However, reasonable results are obtained from 875 to 900 MHz, where the antenna mode scattering dominates: the resistance follows the simulated value in magnitude and shape. On the other hand, the coaxial measurement does not give similar results. Because the PIFA does not have an infinite ground plane, it is not ideally a single-ended structure: connecting the feed line outer conductor to the ground plane induces currents to the outer conductor, which leads to higher dissipation, and thus higher measured antenna resistance.

The reactance hits almost exactly the opposite reactance of 1 pF, and the coaxial measurement results. The simulated value is further away from the measured values, but the simulated value cannot be considered a perfect reference for the scattering measurement: the reactances of 3D antenna structures calculated with HFSS often differ from results of other simulators (e.g., [13]). However, HFSS allows true 3D modelling without infinite layers, which allows the study of ground plane size in small PIFA antennas.

In the measurement of the PIFA antenna, the scattering technique evidently has two problems: First, the PIFA is a complicated three-dimensional system, which is probably not described well enough by a simple series resistance and reactance model, as is supposed in [1] and [2] as the theory of scattering is developed. The structural mode is also high in magnitude (by a factor of four in the scattering parameter higher than with the Palomar antenna), and complex in frequency, as with patches [14]. Taking into account the polarization coupling in the antenna, like in [4], would probably give better results. Second, the error estimates cannot describe the error due to too simple an antenna model. Thus only a small value of error is presented, even if the resistance is negative.

VI. CONCLUSION

This paper presented a scattering technique for antenna input impedance measurements of reactive antennas. Theory was developed and sources of measurement error considered. Two reactive antennas were measured at UHF frequencies. From the error analysis and the measurements, it was seen that the technique gives the best results when the antenna mode dominates the structural mode scattering.

The measurements of the Palomar antenna, a modified dipole, justified the theoretical construction; the results of the measurements and the simulations of the antenna coincided well. The results of the PIFA antenna were more complicated. The structural mode of the PIFA antenna is high in magnitude, and the used model is too simple to describe the scattering of this three-dimensional antenna accurately. Nevertheless, reasonable results were acquired, where the antenna mode scattering dominated the structural mode.

The measurement technique proved to be valid in a narrow band, about three times the half-power bandwidth of the antenna. However, this was achieved with very simple apparatus: a vector signal analyzer and a GTEM cell, which could be replaced with an antenna and an anechoic chamber. No compensation or background elimination techniques other than averaging and scattering parameter reduction in the VNA were used. The simplicity of the apparatus and the measurements makes the technique advantageous in narrow band measurements.

ACKNOWLEDGMENT

The authors wish to thank M. Hirvonen for many useful discussions on antenna scattering, and C. Icheln and the Radio Laboratory of Helsinki University of Technology for cooperation and the opportunity to use the GTEM cell

REFERENCES

[1] D. D. King, "Measurement and interpretation of antenna scattering," *Proc. IRE*, vol. 37, pp. 770–777, Jul. 1949.
[2] R. F. Harrington, "Theory of loaded scatterers," *Proc. Inst. Elect. Eng.*, vol. 111, pp. 617–623, Apr. 1964.
[3] J. T. Mayhan, A. R. Dion, and A. J. Simmons, "A technique for measuring antenna drive port impedance using backscatter data," *IEEE Trans. Antennas Propag.*, vol. 42, pp. 526–532, Apr. 1994.
[4] W. Wiesbeck and E. Heidrich, "Wide-band multiport antenna characterization by polarimetric RCS measurements," *IEEE Trans. Antennas Propag.*, vol. 46, pp. 341–350, Mar. 1998.
[5] P. V. Nikitin and K. V. S. Rao, "Theory and measurement of backscattering from RFID tags," *IEEE Antennas Propag. Mag.*, vol. 48, pp. 212–218, Dec. 2006.
[6] P. Pursula, M. Hirvonen, K. Jaakkola, and T. Varpula, "Antenna effective aperture measurement with backscattering modulation," *IEEE Trans. Antennas Propag.*, vol. 55, no. 10, pp. 2836–2843, Oct. 2007.
[7] E. F. Knott, J. F. Schaeffer, and M. T. Tuley, *Radar Cross Section*. Boston, MA: Artech House, 1993, pp. 407–407.
[8] C. Icheln, "The construction and application of a GTEM cell," Master's thesis, Faculty of Electrical Engineering, Technical Univ. Hamburg, Hamburg, Germany, Nov. 1995.
[9] C. Icheln, P. Haapala, and P. Vainikainen, "Application of a GTEM cell to small antenna measurements," in *IEEE AP-S Int. Symp. Digest*, Montreal, Canada, Jul. 1997, vol. 1, pp. 546–549.
[10] P. Hui, "Small antenna measurements using a GTEM cell," in *Proc. IEEE Antennas and Propagation Society Int. Symp.*, Jun. 2003, vol. 4, pp. 715–718.
[11] The Palomar Project, Passive Long Distance Multiple Access UHF RFID System Public Rep., European Commission, Project IST1999-10339, Nov. 2002.
[12] M. Hirvonen, P. Pursula, K. Jaakkola, and K. Laukkanen, "Planar inverted-F antenna for radio frequency identification," *Electron. Lett.*, vol. 40, pp. 848–850, Jul. 2004.
[13] W. Yu, J. Yeo, and R. Mittra, "Application of non-uniform and conformal FDTD techniques to the analysis of a class of planar antennas," in *Proc. IEEE Antennas and Propagation Society Int. Symp.*, Jun. 2002, vol. 2, p. 675, Fig 1.
[14] E. Newman and D. Forrai, "Scattering from a microstrip patch," *IEEE Trans. Antennas Propag.*, vol. 35, pp. 245–251, Mar. 1987.
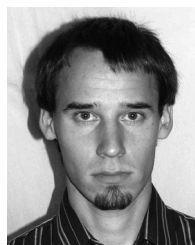
Pekka Pursula was born in Vantaa, Finland, in 1978. He received the Master of Science (Tech.) degree (with distinction) in technical physics from Helsinki University of Technology (TKK), Espoo, Finland, in 2002.

In 2002, he was with Philips Medical Systems Finland developing RF systems in magnetic resonance imaging. Since 2003, he has been with the Technical Research Centre of Finland (VTT), Espoo. He is co-inventor of two international patent applications. His present research interests include RFID systems and wireless sensors.

Mr. Pursula received the Young Scientist Award at the URSI/IEEE XXIX Convention on Radio Science, Espoo, in November 2004.

Dan Sandström is working toward the M.Sc. degree in electrical engineering at Helsinki University of Technology (TKK), Espoo, Finland.

From 2005 to 2007, he was a Research Assistant in the Technical Research Centre of Finland (VTT), Espoo. He is currently with the Electronic Circuit Design Laboratory, TKK. His research interests involve millimeter-wave integrated circuit design in CMOS.

Kaarle Jaakkola was born in Helsinki, Finland, in 1976. He received the Master of Science (Tech.) degree in electrical engineering from Helsinki University of Technology (TKK), Espoo, Finland, in 2003.

Since 2000, he has been working with the Technical Research Centre of Finland (VTT), Espoo, first as a Research Trainee and from 2003 on as a Research Scientist. From 2000 to 2002, he participated in the Palomar (EC IST) project developing RF parts for a new RFID system. His current research interests include RFID systems, wireless and applied sensors, antennas, electromagnetic modelling, and RF electronics.